Switching Mechanics with Chemistry: A Model for the Bending Stiffness of Amphiphilic Bilayers with Interacting Headgroups in Crystalline Order

Markus A. Hartmann,[1] Richard Weinkamer,[1] Thomas Zemb,[2] Franz Dieter Fischer,[3] and Peter Fratzl[1,*]

[1]*Max Planck Institute of Colloids and Interfaces, Am Mühlenberg 1, D-14476 Potsdam, Germany*
[2]*LIONS at DRECAM/SCM, C.E.A. Saclay, F-91191 Gif sur Yvette, France*
[3]*Institute of Mechanics, Montanuniversität Leoben, Franz-Josef Straße 18, A-8700 Leoben, Austria*

(Received 21 November 2005; published 7 July 2006)

Bilayer structures in catanionic systems experimentally showed peculiar mechanical behavior. The observed increase in the bending stiffness is supposedly connected to additional hydrogen bonds forming between anionic headgroups. With a simple model, we can explain the extreme sensitivity of the bending stiffness of the membrane on the molar ratio of the charged molecules. This effect is further amplified by the sandwichlike structure of the membrane, where the apolar core separating the headgroups acts via a kind of lever-arm principle. As a consequence of these combined effects, the model membrane changes from a soft behavior with bending rigidities on the order of $10k_BT$ to an extremely stiff membrane with a bending stiffness more than 2 orders of magnitude larger where most of this change occurs within a molar ratio interval smaller than 0.1.

DOI: 10.1103/PhysRevLett.97.018106 PACS numbers: 87.16.Dg

Amphiphilic molecules are well known for their ability to self-assemble into ''films'' with defined area, stiffness, and curvature [1]. These films assemble into complex geometrical structures, such as micelles, vesicles, ''sponge'' or lamellar phases when dissolved in water [2]. The chemical potential of any surfactant assembly can be expressed as a function of the integrated average curvature, the so-called packing parameter, and the area per headgroup. When a configuration of zero average curvature is stablest, amphiphiles form bilayer structures stacked in smectic order—usually in multilayered vesicles [3,4]. For a membrane composed of a mixture of two amphiphiles with oppositely charged headgroups [5], the lateral cohesion energy of the bilayer is much stronger than of all other known types of bilayers. This so-called ''catanionic'' system [6] off stoichiometry and in the absence of excess salt, i.e., ''true catanionics,'' shows very peculiar behavior, such as fragmentation of lamellae upon dilution into micron-sized rigid nanodisks [7]. Measurements of the mechanical properties of these nanodisks yielded bending rigidities of the order of hundreds to thousands k_BT, i.e., at least 2 orders of magnitude larger than electrically charged bilayers [8]. Another special feature of true catanionics is the extreme sensitivity of the phase diagram with respect to the molar ratio between anionic and cationic surfactants. While at equimolar ratio, only concentrated liquid crystals are formed, close to molar ratios $1/3$ or $2/3$, large domains of colloidal stability can be observed, e.g., cylindrical micelles, punctuated planes, and polyhedra, respectively [9,10]. These systems show the highest bending stiffness yet reported for a self-assembled system based upon surfactants, indicated by giant colloids which are molecularly flat over a length of 10 micrometers and more and, therefore, are observable directly under the optical microscope. Except for the case of catanionics, direct measurements of the mechanical properties of bilayers are scarce. This is because, first, due to line defects, $P_{\beta'}$-type phases are a very brittle material. Second, most phases in the L_β state or with tilted chains are metastable only. Critically compiled data can be found in Chap. 5 of Ref. [11]. The most reliable experiment on a single frozen membrane composed of zwitterionic lipids has been published recently [12]. These peculiar experimental observations motivate our modeling and exploration of the mechanical properties of bilayers made of amphiphilic molecules with oppositely charged headgroups occupying a triangular lattice. The important lateral interactions to be modeled are of electrostatic origin and, additionally, a probably dominant hydrogen bond frequently observed between parallel carboxylates [13]. The formation of these additional bonds between anionic headgroups is modeled by a spring network. Our model therefore displays some resemblance to models of the membrane-associated cytoskeleton of living cells, e.g., of erythrocytes [14].

On a mesoscopic scale, our model membrane as sketched in Fig. 1 consists of an apolar core with a width h and an upper and lower charged layer formed by the

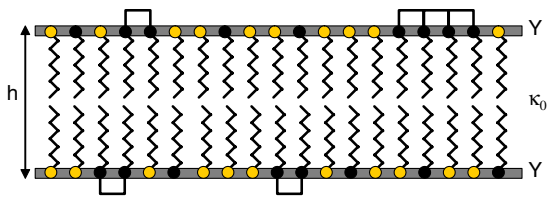

FIG. 1 (color online). A cut through a lipid bilayer membrane. The two differently charged headgroups are shown as dark (anionic) and light circles (cationic), respectively. The black bars connecting two neighboring anionic molecules indicate the formation of additional bonds (e.g., hydrogen bonds).

headgroups of the molecules. The mechanical behavior of the membrane is described by the bending stiffness of the apolar core κ_0, and the in-plane stiffness of the charged layers represented by their in-plane tension modulus Y, i.e., the two-dimensional analog of the modulus of elasticity E (Y is therefore measured in units of force/length). Because of the sandwich structure, the bending stiffness κ of the whole membrane is given by [15]

$$\kappa = \kappa_0 + \frac{h^2}{2} Y. \tag{1}$$

Different from the reported h^2 dependence of κ_0 [11], the same dependence for the second term is simply the result of the sandwich structure. With our model, we want to understand the effect of additional bonds between the headgroups on Y and, consequently, on the mechanical behavior of the whole membrane, when the electrostatic contribution is much smaller. The experimental scenario we model is a fluid membrane where the oppositely charged headgroups arrange themselves according to the thermodynamic equilibrium at temperature T. Because of a change in the solvent conditions, the configuration of molecular heads ''freezes'' and additional bonds between the headgroups develop. In the microscopic part of the model, the closely packed molecules with either positively or negatively charged headgroups occupy a triangular lattice with lattice spacing a. The electrostatic interactions between the charged heads are described by nearest neighbor interactions only using a standard Ising model [16]. The sign of the exchange energy J is chosen to ensure an antiferroelectric ordering between the charged heads [17]. An equilibrium configuration of the positively and negatively charged heads is obtained using standard Monte Carlo techniques [18]. This equilibrium configuration is then fixed, and nearest neighbors are assumed to be connected by linear elastic springs. Two nearest neighbor molecules with negative charge are assigned a spring constant k_1; all other headgroup pairs are connected by springs with $k_2 \ll k_1$.

The mechanical properties of the layers can be described by a stiffness matrix relating the in-plane normal tensions σ_1 and σ_2 and the in-plane shear tension τ (all measured in units of force/length) to the in-plane strains ϵ_1 and ϵ_2 and the in-plane shear angle γ.

$$\begin{pmatrix} \sigma_1 \\ \sigma_2 \\ \tau \end{pmatrix} = \begin{pmatrix} Q_{11} & Q_{12} & Q_{13} \\ Q_{12} & Q_{22} & Q_{23} \\ Q_{13} & Q_{23} & Q_{33} \end{pmatrix} \begin{pmatrix} \epsilon_1 \\ \epsilon_2 \\ \gamma \end{pmatrix}. \tag{2}$$

The six independent entries of the stiffness matrix were determined by performing three independent computational mechanical tests by imposing different deformations on the system and taking care of appropriate boundary conditions. Using a Monte Carlo algorithm, the position of the molecules in elastic equilibrium was determined. Then the elastic coefficients were calculated, yielding

$$Q_{11} - Q_{22} \approx Q_{13} \approx Q_{23} \approx Q_{11} - Q_{12} - 2Q_{33} \approx 0, \tag{3}$$

for all molar ratios. Thus, the layers show isotropic elastic behavior, and, therefore, the number of independent elastic parameters can be reduced to two only, the tension modulus Y and the two-dimensional Poisson ratio ν,

$$Y = Q_{11}(1 - \nu^2), \qquad \nu = \frac{Q_{12}}{Q_{11}}. \tag{4}$$

The connection to the widely used area compression modulus K_A [11] reads as

$$K_A = \frac{Q_{11}(1 + \nu)}{2} = \frac{Y}{2(1 - \nu)}. \tag{5}$$

For the numerical simulations, we chose for the geometry of the membrane a thickness of the apolar core $h =$ 3 nm [7]. For the bending stiffness of the apolar core, values ranging from 3 to $50 k_B T$ have been reported [11]; our choice was $\kappa_0 = 10 k_B T$. The electrostatic contribution to κ_0 has been shown to lie in the range of some $k_B T$ [19,20]. As will be shown, this contribution is negligible to the increase in bending stiffness induced by the additional bonds between anionic headgroups. To study the influence of the ordering due to the electrostatic interaction between the headgroups, simulations were performed with two different values for the Ising exchange energy J, $J = 1 k_B T$ and $J = 0$, the latter corresponding to a random arrangement of the molecules. The binding energy of the additional hydrogen bonds is about $2 k_B T$ [21]. To transform this energy into a value for the spring constant k_1, we consider a Lennard-Jones potential with an equal binding energy and an equilibrium spacing $a = 0.8$ nm. A Taylor expansion gives for the harmonic term

$$k_1 \approx \frac{72W}{a^2} = 180 k_B T/\mathrm{nm}^2 \approx 4.5\ \mathrm{eV}/\mathrm{nm}^2. \tag{6}$$

The spring constant between the other headgroup pairs should be orders of magnitude smaller so that the contribution of the apolar core κ_0 dominates in the case without additional bonds. We set $\gamma = k_1/k_2 = 10^4$.

Membranes with a different composition of anionic and cationic molecules have been studied covering the whole molar ratio range from pure cationic ($c_A = 0$) to pure anionic layers ($c_A = 1$). The choice $J = 1 k_B T$ resulted in the tendency that anionic molecules try to be surrounded by cationic ones and vice versa. For sufficiently large molar ratios, a continuous network of additional bonds emerges with holes due to the presence of dispersed cationic molecules [Fig. 2(a)]. For molar ratios c_A close to $2/3$, a regular superlattice is formed [Fig. 2(b)]. The honeycomb structure is due to a cationic molecule surrounded by six anionic molecules. For small molar ratios, the network of additional bond breaks into separated islands of additional bonds [Fig. 2(c)].

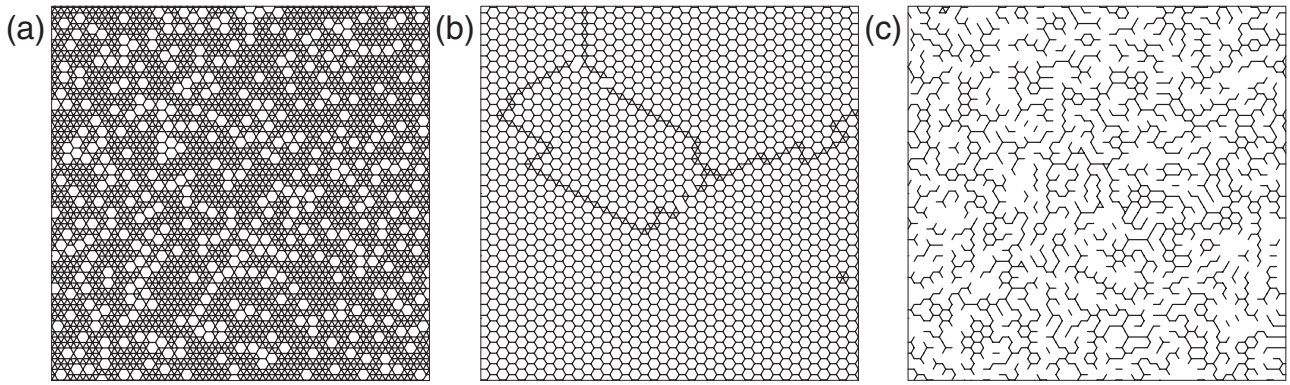

FIG. 2. Three typical configurations for different molar ratios and a temperature of $J/k_BT = 1$ are plotted for (a) $c_A = 0.9$, (b) $c_A = 0.67$, and (c) $c_A = 0.5$, respectively. The additional bonds between anionic molecules are marked by small bars.

Figure 3 summarizes our results concerning the mechanics of the model membrane as a function of its composition. Plotted are the tension modulus Y, the two-dimensional Poisson ratio ν, and the bending stiffness κ, together with the effective elastic modulus $\bar{E}$, defined as $\bar{E} = [12(1 - \nu^2)/h^3]\kappa$, with $\nu = 1/3$. The two different curves allow a comparison between the case where the electrostatic interaction between the charged headgroups results in an ordering of the molecules and the case of a random arrangement of the molecules. For both Y and κ, the general behavior is characterized by a transition over several orders of magnitude from low to high values, when the molar ratio is increased. Significant differences between the ordered and the random cases occur only in the range between $c_A = 0.6$ and $c_A = 0.8$ where the transition substantially takes place. The effect of the order consists in postponing the transition to higher molar ratios and therefore steepening the switching from soft to stiff. In this range $c_A = 0.6$–0.8, the two-dimensional Poisson ratio ν takes values close to 1 in the case of ordering, while it is roughly $1/3$ for all molar ratios in the random case, which is the exact value for an isotropic two-dimensional solid, if the Cauchy relation is valid [22]. The calculated values of κ lie in the range of 10–$1000 k_BT$, while the effects on κ_0 [see Eq. (1)] due to electrostatic interactions such as deformation of the counterion cloud may add some rigidity in the range 1–$10 k_BT$ [19,20,23]. Thus, these effects are at least 1 order of magnitude smaller than the chemical effects considered in this Letter, leading to unexpected high in-plane persistence lengths [8,24].

In some limiting cases, analytical results can be obtained, which are in full agreement with the computational results. For a pure anionic configuration ($c_A = 1$), the only springs present are that of type k_1 and the triangular lattice is mechanically described by $Y = 2/\sqrt{3}k_1$ and $\nu = 1/3$. Hence, the additional bonds increase the bending modulus by $\Delta\kappa = h^2 k_1/3$, resulting in a maximum stiffness of the membrane of $\approx 910 k_BT$. For a completely ordered lattice, which can be formed for $c_A = 2/3$, the stiff bonds form a honeycomb lattice [see Fig. 2(b)] and ν is given by $2(\gamma^2 + \gamma + 1)/(2\gamma^2 + 11\gamma + 5)$, $\gamma = k_1/k_2$. In the limit $\gamma \to \infty$, then $\nu \to 1$ and, therefore, with Eq. (4), $Y \to 0$, reflecting that a honeycomb lattice is a kinematically undetermined structure that can be stretched or sheared without stretching any bond. To understand the transition between soft and stiff, the percolation properties of the network of addi-

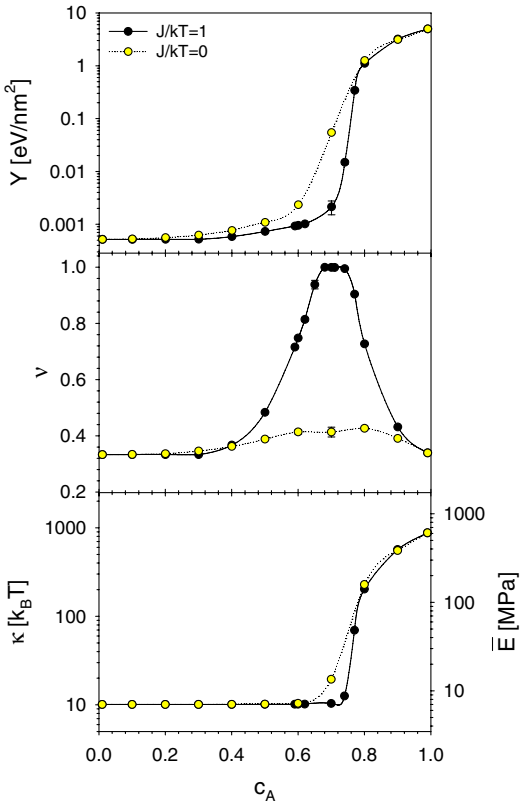

FIG. 3 (color online). Tension modulus Y (top), two-dimensional Poisson ratio ν (middle) of the headgroup region, and the bending stiffness κ, as well as the (effective) elastic modulus $\bar{E}$ (bottom) of the complete sandwich structure plotted as a function of composition. The behavior for two different temperatures is shown ($J/k_BT = 1$ and $= 0$, respectively). The lines drawn are guides to the eyes. Note the semilogarithmic scale in the plots at the top and bottom.

tional bonds are crucial. The site percolation threshold for a triangular lattice is given by $c_A = 0.5$ [25]. Since the conductivity backbone contains quasi-one-dimensional structures which do not resist deformation [26], the formation of a rigid backbone is essential for the stiffening [27]. The rigidity percolation on the (random) triangular lattice was found to occur around a bond probability $p_{ce} = 0.65$ [28]. This corresponds to a rigidity percolation at a site concentration $c_A = 0.81$, but for our case this value is too high, since a random arrangement of atoms is not equivalent to a random arrangement of bonds. In the case of an electrostatic ordering between the molecules, the onset of the rigidity percolation is postponed to high values of c_A. First, the ordering opposes the formation of additional bonds. Second, in the honeycomb framework of the additional bonds, each honeycomb cell is kinematically undetermined. Beyond a concentration of $c_A = 2/3$ in the case of full order, each additional anionic atom placed in the center of a honeycomb cell causes the formation of six additional bonds and the cell becomes stiff. The stiffening effect of the charged layer is reflected in the behavior of the bending stiffness κ only when the stiffening of the surface bonds markedly exceeds κ_0, which happens beyond $c_A = 0.65$ (Fig. 3). The energies of the additional microscopic bonds are rather low; however, the stiffening effect is tremendously enhanced as a result of the sandwichlike structure of the membrane [Eq. (1)].

Although the specificities of the experiments are not captured in our model, two main experimental observations make us confident that the mechanism, which allows the model membrane to change the mechanical properties in a very narrow concentration range, is also acting in real catanionic systems. First are the high bending rigidities observed in nanodisks and in polyeders, where $500 k_B T$ has been found as a lower bound [8]. Second, the high sensitivity of the system to small changes in the molar ratio between cations and anions in certain concentration ranges. This sensitivity could also be the reason for the intriguing coexistence of facetted and unfacetted bent spheres which can be observed in freeze fracture microscopy. This has been up to now considered as an artifact or due to the presence of impurities. In the case when the molar ratio is around the stiffening transition, local fluctuations in the composition, which can be as large as 10% [29], can be responsible for finding colloids with mechanical stiffness varying 1 order of magnitude in the same sample, unfacetted soft and facetted stiff colloids.

We acknowledge support from the French-German network "Complex fluids in thin films."

*Electronic address: Peter.Fratzl@mpikg.mpg.de

[1] S. Hyde, *The Language of Shape* (Elsevier, Amsterdam, 1997).
[2] T. N. Zemb, Colloids Surf. A **130**, 435 (1997).
[3] J. N. Israelachvili, D. J. Mitchell, and B. W. Ninham, J. Chem. Soc., Faraday Trans. 2 **72**, 1525 (1976).
[4] M. Dubois and T. Zemb, Curr. Opin. Colloid Interface Sci. **5**, 27 (2000).
[5] H. Fukuda, K. Kawata, H. Okuda, and S. L. Regen, J. Am. Chem. Soc. **112**, 1635 (1990).
[6] P. Jokela, B. Jönsson, B. Eichmüller, and K. Fontell, Langmuir **4**, 187 (1988).
[7] T. Zemb, M. Dubois, B. Deme, and T. Gulik-Krzywicki, Science **283**, 816 (1999).
[8] M. Dubois, T. Gulik-Krzywicki, B. Deme, and T. Zemb, C.R. Acad. Sci. Ser. IIc **1**, 567 (1998).
[9] M. Dubois, B. Deme, T. Gulik-Krzywicki, J. C. Dedieu, C. Vautrin, S. Desert, E. Perez, and T. Zemb, Nature (London) **411**, 672 (2001).
[10] T. Zemb and M. Dubois, Aust. J. Chem. **56**, 971 (2003).
[11] D. Boal, *Mechanics of the Cell* (Cambridge University Press, Cambridge, England, 2002).
[12] J. Daillant, E. Bellet-Amalric, A. Braslau, T. Charitat, G. Fragneto, F. Graner, S. Mora, and F. Rieutord, Proc. Natl. Acad. Sci. U.S.A. **102**, 11 639 (2005).
[13] M. L. Lynch, Y. Pan, and R. G. Laughlin, J. Phys. Chem. **100**, 357 (1996).
[14] S. K. Boey, D. H. Boal, and D. E. Discher, Biophys. J. **75**, 1573 (1998).
[15] L. D. Landau and E. M. Lifschitz, *Elastizitätstheorie* (Akademie Verlag, Berlin, 1991).
[16] R. Weinkamer, P. Fratzl, B. Sepiol, and G. Vogl, Phys. Rev. B **58**, 3082 (1998).
[17] M. K. Phani, J. L. Lebowitz, M. H. Kalos, and O. Penrose, Phys. Rev. Lett. **45**, 366 (1980).
[18] R. Weinkamer, P. Fratzl, H. S. Gupta, O. Penrose, and J. L. Lebowitz, Phase Transit. **77**, 433 (2004).
[19] M. Winterhalter and W. Helfrich, J. Phys. Chem. **92**, 6865 (1988).
[20] P. Pincus, J.-F. Joanny, and D. Andelmann, Europhys. Lett. **11**, 763 (1990).
[21] S. Zhu, M. Heppenstall-Butler, M. F. Butler, P. D. A. Pudney, D. Ferdinando, and K. J. Mutch, J. Phys. Chem. B **109**, 11 753 (2005).
[22] M. Born and K. Huang, *Dynamical Theory of Crystal Lattices* (Clarendon, Oxford, 1988).
[23] G. Brotons, M. Dubois, L. Belloni, I. Grillo, T. Narayanan, and T. Zemb, J. Chem. Phys. **123**, 024704 (2005).
[24] M. Dubois, V. Lizunov, T. Gulik-Krzywicki, J. M. Verbavatz, E. Perez, J. Zimmerberg, and T. Zemb, Proc. Natl. Acad. Sci. U.S.A. **101**, 15 082 (2004).
[25] S. C. van der Marck, Phys. Rev. E **55**, 1514 (1997).
[26] S. Feng, B. I. Halperin, and P. N. Sen, Phys. Rev. B **35**, 197 (1987).
[27] A. R. Day, R. R. Tremblay, and A. M. S. Tremblay, Phys. Rev. Lett. **56**, 2501 (1986).
[28] M. Sahimi and J. D. Goddard, Phys. Rev. B **32**, 1869 (1985).
[29] M. Dubois, L. Belloni, T. Zemb, B. Deme, and T. Gulik-Krzywicki, Prog. Colloid Polym. Sci. **115**, 238 (2000).